Cerebral Cortex, September 2021;31: 4169–4179

https://doi.org/10.1093/cercor/bhab076
Advance Access Publication Date: 7 April 2021
Original Article

ORIGINAL ARTICLE

Myeloarchitectonic Asymmetries of Language Regions in the Human Brain

Di Yuan[1,2], Daiyi Luo[1,2], Veronica P. Y. Kwok[2], Yulong Zhou[1,2], Haoyue Tian[1,2], Qianqian Yu[2], Jie An[3], Jia-Hong Gao[4,5], Shijun Qiu[3] and Li Hai Tan[1,2]

[1]Guangdong-Hongkong-Macau Institute of CNS Regeneration and Ministry of Education CNS Regeneration Collaborative Joint Laboratory, Jinan University, Guangzhou 510632, China, [2]Center for Language and Brain, Shenzhen Institute of Neuroscience, Shenzhen 518060, China, [3]Department of Radiology, First Affiliated Hospital of Guangzhou University of Chinese Medicine, Guangzhou 510400, China, [4]McGovern Institute for Brain Research, Peking University, Beijing, China and [5]Center for MRI Research, Peking University, Beijing 100871, China

Address correspondence to Dr. Li Hai Tan. Email: tanlh@sions.cn, Dr. Shijun Qiu. Email: qiu-sj@163.com, or Dr. Jia-Hong Gao. Email: jgao@pku.edu.cn

Abstract

One prominent theory in neuroscience and psychology assumes that cortical regions for language are left hemisphere lateralized in the human brain. In the current study, we used a novel technique, quantitative magnetic resonance imaging (qMRI), to examine interhemispheric asymmetries in language regions in terms of macromolecular tissue volume (MTV) and quantitative longitudinal relaxation time (T1) maps in the living human brain. These two measures are known to reflect cortical myeloarchitecture from the microstructural perspective. One hundred and fifteen adults (55 male, 60 female) were examined for their myeloarchitectonic asymmetries of language regions. We found that the cortical myeloarchitecture of inferior frontal areas including the pars opercularis, pars triangularis, and pars orbitalis is left lateralized, while that of the middle temporal gyrus, Heschl's gyrus, and planum temporale is right lateralized. Moreover, the leftward lateralization of myelination structure is significantly correlated with language skills measured by phonemic and speech tone awareness. This study reveals for the first time a mixed pattern of myeloarchitectonic asymmetries, which calls for a general theory to accommodate the full complexity of principles underlying human hemispheric specialization.

Key words: asymmetry, language, microstructure, myelination, qMRI

Introduction

Research on Broca's and Wernicke's aphasia resulting from cerebral damage indicates that language processing is predominantly accomplished by the left hemisphere of the human brain (Broca 1861; Wernicke 1969). This observation has been corroborated by various kinds of brain asymmetry studies with respect to both brain structure and brain function (Hugdahl and Westerhausen 2010; Bishop 2013).

The structure indices of brain asymmetry include microstructural features and macroscopic dimensions. The microstructural studies focus on the number and density of cells, number of spines, degree of arborization of dendrites, and axons, which usually require postmortem analysis and histological sections (Amunts 2010). For example, Amunts et al. (1999) measured the cell densities of 10 human brains in serial histological sections stained for cell body. They found that area 44, which belongs to Broca's area, was left lateralized in all brains. Uylings et al. (2006) reported a left-lateralized neuron density in Nissl-stained sections of area 44 from 10 adult brains and that the lateralization value of five male brains reached a significant level. Using DiI tract-tracing, a tracing method with a fluorescent lipophilic cationic indocarbocyanine dye, Galuske et al. (2000) demonstrated the inter-hemisphere asymmetry of interconnectivity within area 22, a site known to play an important role during auditory signal processing. They found that although the cluster diameter of area 22 was similar in both hemispheres, their spacing was about 20 percent larger in the left hemisphere implying more neuropil could be included in the left than in the right to support language functions. Subsequent research replicated the stronger connectivity in the left hemisphere by indicating that the size of pyramidal cells in large layer III is larger in regions of the primary and secondary auditory cortex, as larger cell bodies might be needed to support longer axons (Hutsler 2003; Hutsler and Galuske 2003).

The macroscopic studies focus on the shape, volume, size of sulci, gyri, and lobe of brain, which are conducted in vivo or in vitro. For example, Geschwind and Levitsky's autopsy study suggested that the size of planum temporale was larger on the left hemisphere than on the right (Geschwind and Levitsky 1968; Geschwind and Galaburda 1985). Compared to autopsy studies, MRI techniques are well suited to measure the entire morphology of surface and intrasulcal anatomy (Keller et al. 2009), and the left lateralization of language-related brain structure seems to emerge in white as well as gray matter. In an MRI study with 12 participants, the extent of extrasulcal and intrasulcal portions of cortex in anterior speech region (pars opercularis and pars triangularis) and planum temporale were found to be significantly larger in the left hemisphere than in the right (Falzi et al. 1982). Penhune et al. (1996) used a probabilistic mapping method to calculate the volumes of white and gray matter. They found that the white matter volumes of the primary auditory cortex were larger on the left hemisphere than on the right. A VBM-DTI study with 109 participants demonstrated leftward gray matter asymmetry of the planum temporale and Heschl's gyri as well as leftward white matter fractional anisotropy asymmetries of the arcuate fasciculus (Takao et al. 2011).

The language-related brain areas are also suggested to be functionally left lateralized. Most neural activities are localized in the left, rather than right, hemisphere during language tasks. These neural activities emerged at the regions including but not limited to left anterior temporal lobe, medial prefrontal cortex (Pylkkänen 2019), left inferior frontal gyrus (Xue et al. 2005; Xue et al. 2006; Rodd et al. 2015), and left middle fusiform (Liu et al. 2008; Tan et al. 2011). Such lateralization could be established even in childhood (Berl et al. 2014; Olulade et al. 2020). More straightforward evidence comes from inter-hemisphere lateralization studies. For example, brain regions including lateral orbital gyrus, prefrontal dorsolateral region, inferior frontal gyrus, superior and middle temporal gyrus, lateral extrastriate region showed significantly more activation voxels in the left hemisphere than in the right hemisphere during a semantic task (Frost et al. 1999). Moreover, by conducting functional transcranial Doppler-ultrasonography (fTCD), Knecht et al. (2000) compared perfusion changes of the two middle cerebral arteries within the potential language areas during a word generation task. They found that the overall distribution of language lateralization was 7.5% being the right hemisphere and 92.5% being the left hemisphere.

Despite a large number of studies demonstrating the left lateralization in language-related regions, there is evidence indicating otherwise. Wada et al. (1975) found that the surface of pars opercularis and the posterior portion of the pars triangularis together was significantly larger on the right side than on the left side in 100 adult postmortem brains, though a reanalysis of these data by Witelson and Kigar (1988) revealed a non-significant ($P = 0.1$) left-lateralized intrasulcal anatomy of this region. Moreover, a significant rightward asymmetry of the white matter was found below the planum temporale (Barrick et al. 2004). The temporoparietal pathway connecting the superior temporal gyrus to the superior parietal lobule was also right-lateralized (Barrick et al. 2007). People with different dominant hands, ages, or genders showed different patterns of language lateralization (Foundas et al. 1998; Knecht et al. 2000; Uylings et al. 2005; Uylings et al. 2006). In some language tasks, strong neural activities were also found on the right hemisphere, such as superior temporal cortex (Lattner et al. 2005), dorsolateral cortex and orbitobasal (Wildgruber et al. 2005), and fusiform gyrus (Tan et al. 2001; Mei et al. 2015; Yang et al. 2019; Cao et al. 2019) on the right side. Especially, since lexical tone is used to convey grammatical or word meanings in more than half of the world's languages (Yip 2002), the functional anatomy and lateralization of lexical tone processing in speech has been intensively investigated. A bi-lateralized cortical network is shown to mediate speech tone, which involves superior temporal regions, inferior prefrontal regions, and the insula (Gandour et al. 2000; Hsieh et al. 2001; Klein et al. 2001; Wong 2002; Liu et al. 2006; Luo et al. 2006; Ren et al. 2009; Li et al. 2010; Xi et al. 2010; Nan and Friederici 2013; Chang et al. 2014; Yu et al. 2014; Ge et al. 2015; Kwok et al. 2016, 2017; Liang and Du 2018).

In this study, we examined the asymmetry of language regions from a microstructural perspective in living human brains. We used a novel technique—quantitative MRI (qMRI)—to quantitatively estimate the brain macromolecular tissue volume (MTV) and quantitative longitudinal relaxation time (T1) maps (Lutti et al. 2014; Gomez et al. 2017). MTV quantifies myelin volume on the basis that the brain macromolecules are principally cell membranes and proteins, and T1 suggests a mechanism of microstructural variation such as dendrite development, myelination, and oligodendrocytes (Mezer et al. 2013; Lutti et al. 2014; Stüber et al. 2014; Gomez et al. 2017; Luo et al. 2019). Therefore, MTV and T1 quantify cortical myeloarchitecture mapping from the microstructural perspective (Lutti et al. 2014; Gomez et al. 2017). The interhemispheric asymmetries of language regions including pars opercularis (POp), pars triangularis (PTr), pars orbitalis (POr), anterior transverse temporal gyrus (Heschl's gyrus, HG), planum temporale (PT), and middle temporal gyrus (MTG) were examined. Two cohorts of participants from Beijing and Guangzhou were recruited and examined with different MRI scanners to test the reproducibility of any observed lateralization effect(s). To examine the specific functions of those language regions, we tested Beijing participants' language skills to elucidating the myelination-behavior relationship. Based on the literature, we hypothesized that language regions may show a mixed-pattern of laterality from the microstructural perspective and the laterality index of myelination structure is related to language skills. Moreover, since previous studies showed a gender effect on functional and structural asymmetries (Shaywitz et al. 1995; Amunts et al.

Table 1 Demographic information and behavioral performance of participants

	Guangzhou	Beijing
Number of participants	65	50
Mean age	24.0	22
Age range	18 ~ 35	19 ~ 28
Gender	36 M; 29F	19 M; 31F
Phoneme counting task (max = 30)	/	10.6 (4.5)
Phoneme deletion task (max = 30)	/	24.7 (3.7)
Monosyllable task (max = 50)	/	45.1 (5.9)
Bisyllabic words task (max = 50)	/	43.3 (6.1)
Quadrisyllabic Chinese phrases task (max = 50)	/	49.2 (2.0)

1999; Uylings et al. 2006; Bogolepova and Malofeeva 2000, 2001), we also examined whether sex influences lateralization from the microstructural perspective in the current study.

Guangzhou Data

Materials and Methods

Participants

Sixty-five Chinese native speakers were recruited from the colleges in Guangzhou (36 male; 29 female; age 24.0 ± 4.5 y, Table 1). All the participants were strongly right handed as measured by the Handedness Inventory (Snyder and Harris 1993), with normal or correct-to-normal vision, and with no history of psychiatric or neurological disorders. They gave informed consent before the experiment and were each paid after the experiment. The study was approved by the ethics committee at the Shenzhen Institute of Neuroscience and in accordance with the Declaration of Helsinki.

Quantitative MRI Data Acquisition

QMRI measurements were guided by the protocols in Mezer et al. (2013, 2016) and Oishi et al. (2018). MRI data were measured by 3 T Siemens Magnetom Prisma scanner (Siemens Healthcare, Erlangen, Germany) with a 64-channel head coil. The quantitative MTV and T1 values were measured from spoiled gradient echo (SPGE) images with flip angles of 4°, 10°, 20°, and 30° (TR = 12 ms, TE = 2.41 ms) at an in-plane resolution of 1×1 mm^2 with a slice thickness of 1 mm. Four spin-echo inversion recovery (SEIR) images were also scanned, with an echo-planar imaging (EPI) read-out, a slab inversion pulse, and spectral fat suppression, to remove field inhomogeneities. The images were collected with inversion times of 50, 200, 400, 1200, and 2400 ms (TE = 49 ms, TR = 3000 ms) at an in-plane resolution of 2.2×2.2 mm^2 with a slice thickness of 4 mm.

QMRI Data Analysis

Both SPGE images and SEIR images were processed by using the mrQ software package (https://github.com/mezera/mrQ) to generate maps of macromolecular tissue volume (MTV) and quantitative T1 for each participant. SPGE images and low-resolution unbiased T1 maps derived from SEIR images were combined (Barral et al. 2010) to estimate the unbiased T1 maps and proton density maps (Fram et al. 1987). MTV maps were calculated from proton density maps. MTV quantifies the non-water volume in each voxel, and the complementary volume is water (cerebrospinal fluid was approximated to water). T1-weighted images were transformed into cortical surface using Freesurfer 6.0 recon-all procedure (Reuter et al. 2012). They were spatially matched with MTV maps and had excellent gray/white matter contrast.

Destrieux atlas in FreeSurfer was used to automatically label the cortex (Destrieux et al. 2010). The boundaries of the labels are customized to each participant based on curvature statistics stored in the ROI atlas. Such a method to parcellate the cortex has been validated using a jackknifing procedure (Fischl et al. 2004). Destrieux atlas has 74 ROIs on each hemisphere. In the current study, twelve regions of interest (ROIs) were selected with six ROIs at each hemisphere: pars opercularis (POp), pars triangularis (PTr), pars orbitalis (POr), anterior transverse temporal gyrus (Heschl's gyrus, HG), planum temporale (PT), and middle temporal gyrus (MTG), as shown in Figure 1. Among them, POp and PTr constitute the conventional Broca's area, which, along with MTG, are essential sites of language functions (Bishop 2013; Tremblay and Dick 2016). HG and PT were chosen as widely known anatomically asymmetric language-relevant regions (Dorsaint-Pierre et al. 2006; Greve et al. 2013). The planum temporale in the Destrieux atlas includes both the posterior horizontal segment and the posterior ascending ramus (i.e. PP). Researchers have demonstrated that these areas are cytoarchitectonically or functionally homogeneous (Steinmetz et al. 1989; Witelson et al. 1995; Binder et al. 1996). For each participant, 'mri_convert' command was used to convert the individual labeled template into the native MTV space. Then, mean MTV and T1 values across voxels within ROI for each participant were computed.

Statistical Analysis

The Laterality Index (LI) was used to quantify the standardized difference of MTV or T1 between left and right hemispheres. The formula is as follows:

$$LI = \frac{(LH - RH)}{(LH + RH)} \tag{1}$$

Where LH is the MTV or T1 from the left hemisphere and RH is the MTV or T1 from the right hemisphere. LI ranges from −1 (completely right lateralized) to +1 (completely left lateralized). A Wilcoxon signed-rank test with false discovery rate (FDR) correction (Benjamini–Hochberg procedure, Benjamini and Hochberg 1995) was used at each ROI to examine the difference between LI and zero. We also measured the percentage of (LH-RH)/RH which refers to the magnitude of the difference between the left side and the right side (Galuske et al. 2000). A Wilcoxon signed-rank test with FDR correction was used at each ROI to examine the difference percentage and zero. The

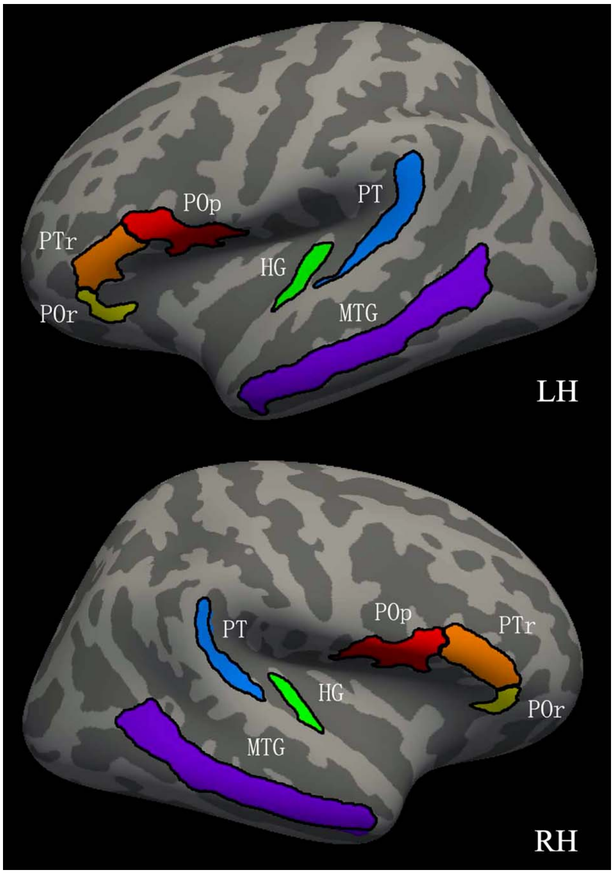

Figure 1. The location of selected ROIs on an inflated cortical surface. The yellow area represents pars orbitalis; the orange area represents pars triangularis; the red area represents pars opercularis; the green area represents Heschl's gyrus; the blue area represents planum temporale; the purple area represents middle temporal gyrus. LH, left hemisphere; RH, right hemisphere.

95% confidence interval (95% CI) and effect size were calculated. The gender effect of lateralization measurements (i.e. LI and difference percentage) was examined by the Mann–Whitney U test.

Results

Mean MTV and T1 values across voxels within each ROI are shown in Table 2. We begin with the one sample Wilcoxon signed-rank test with false discovery rate (FDR) correction at each ROI to examine the difference between LI of MTV and zero. LIs of MTV were significantly larger than zero in inferior frontal areas including the POp [$Z = 3.510$, $p_{corr} = 0.0004$, $M = 0.0066$, $SD = 0.0230$, 95%CI = [0.0009, 0.0123], effect size = 0.44], PTr [$Z = 5.846$, $p_{corr} < 0.0001$, $M = 0.0224$, $SD = 0.0228$, 95%CI = [0.0167, 0.0280], effect size = 0.73], and POr [$Z = 6.192$, $p_{corr} < 0.0001$, $M = 0.0428$, $SD = 0.0385$, 95%CI = [0.0333, 0.0524], effect size = 0.77], while they were significantly smaller than zero in temporal areas including the MTG [$Z = -4.129$, $p_{corr} < 0.0001$, $M = -0.0120$, $SD = 0.0219$, 95%CI = [−0.0174, −0.0066], effect size = 0.51], HG [$Z = -5.947$, $p_{corr} < 0.0001$, $M = -0.0156$, $SD = 0.0144$, 95%CI = [−0.0192, −0.0120], effect size = 0.74], and PT [$Z = -5.494$, $p_{corr} < 0.0001$, $M = -0.0192$, $SD = 0.0269$, 95%CI = [−0.0258, −0.0125], effect size = 0.68] (see Fig. 2A).

We then calculated LIs of T1 to examine whether this cortical myeloarchitectonic mapping would show a similar lateralization pattern as MTV. LIs of T1 were significantly smaller than zero in inferior frontal areas including the POp [$Z = -3.081$, $p_{corr} = 0.0021$, $M = -0.0033$, $SD = 0.0125$, 95%CI = [−0.0064, −0.0002], effect size = 0.38], PTr [$Z = -5.586$, $p_{corr} < 0.0001$, $M = -0.0126$, $SD = 0.0153$, 95%CI = [−0.0164, −0.0088], effect size = 0.69], and POr [$Z = -6.543$, $p_{corr} < 0.0001$, $M = -0.0262$, $SD = 0.0184$, 95%CI = [−0.0307, −0.0216], effect size = 0.81], but were significantly larger than zero in temporal areas including the MTG [$Z = 5.965$, $p_{corr} < 0.0001$, $M = 0.0107$, $SD = 0.0147$, 95%CI = [0.0070, 0.0143], effect size = 0.74], HG [$Z = 6.582$, $p_{corr} < 0.0001$, $M = 0.0151$, $SD = 0.0108$, 95%CI = [0.0124, 0.0177], effect size = 0.82], and PT [$Z = 6.571$, $p_{corr} < 0.0001$, $M = 0.0152$, $SD = 0.0128$, 95%CI = [0.0120, 0.0183], effect size = 0.82] (see Fig. 2B).

The difference percentage of MTV and T1 showed the same lateralization patterns as LI of MTV and T1 (Fig. S1A&B). Specifically, MTV in Pop, PTr, and POr was 1.4%, 4.7%, and 9.3% larger in left than right hemisphere, respectively [POp: $Z = 3.568$, $p_{corr} = 0.0004$; PTr: $Z = 5.852$, $p_{corr} < 0.0001$; POr: $Z = 6.205$, $p_{corr} < 0.0001$], while MTV in MTG, HG, and PT was 2.3%, 3%, and 3.6% smaller in left than right hemisphere, respectively [MTG: $Z = -4.101$, $p_{corr} < 0.0001$; HG: $Z = -5.957$, $p_{corr} < 0.0001$; PT: $Z = -5.466$, $p_{corr} < 0.0001$]. In addition, T1 in Pop, PTr, and POr was 0.6%, 2.5%, and 5% smaller in left than right hemisphere, respectively [POp: $Z = -3.120$, $p_{corr} = 0.0018$; PTr: $Z = -5.555$, $p_{corr} < 0.0001$; POr: $Z = -6.532$, $p_{corr} < 0.0001$], while T1 in MTG, HG, and PT was 2.2%, 3.1%, and 3.1% larger in left than right hemisphere, respectively [MTG: $Z = 6.022$, $p_{corr} < 0.0001$; HG: $Z = 6.604$, $p_{corr} < 0.0001$; PT: $Z = 6.630$, $p_{corr} < 0.0001$].

Taken together, both MTV and T1 data converge to indicate that the cortical myelination of the POp, PTr, and POr is leftward and that of the MTG, PT, and HG is rightward. Percentages of the individuals in Guangzhou showing the same lateralization pattern ranged from 62% to 90% (Table 3). We also examined gender effects in terms of LI and difference percentage within each ROI by using Mann–Whitney U tests. The results revealed that none of the ROIs showed a significant gender difference ($ps > 0.05$).

Beijing Data

Materials and Methods

Participants

Fifty Chinese were recruited from the colleges in Beijing (19 male; 31 female; age 22 ± 2.1 y, Table 1). They were bilingual in Chinese and English. All the participants were strongly right handed as measured by the Handedness Inventory (Snyder and Harris 1993), with normal or correct-to-normal vision, and with no history of psychiatric or neurological disorders. They gave informed consent before the experiment and were each paid after the experiment.

Quantitative MRI Data Acquisition

QMRI parameters were from the protocols in Mezer et al. (2013, 2016). MRI data were measured by 3 T Discovery MR750 system (General Electric Healthcare Milwaukee, WI, USA) with an 8-channel head coil. The quantitative MTV and T1 values were measured from spoiled gradient echo (SPGE) images with flip angles of 4°, 10°, 20°, and 30° (TR = 14 ms, TE = 2 ms) at an in-plane resolution of 1×1 mm^2 with a slice thickness of 1 mm. To

Table 2 Mean MTV and T1 values across voxels within each ROI

	Left hemisphere				Right hemisphere			
	MTV mean (SD)		T1 mean (SD)		MTV mean (SD)		T1 mean (SD)	
	Male	Female	Male	Female	Male	Female	Male	Female
Guangzhou (N = 65, male = 36, female = 29)								
POp	0.197 (0.011)	0.195 (0.016)	1.461 (0.034)	1.465 (0.061)	0.194 (0.010)	0.194 (0.018)	1.473 (0.027)	1.470 (0.036)
PTr	0.194 (0.012)	0.199 (0.035)	1.455 (0.049)	1.453 (0.080)	0.186 (0.011)	0.190 (0.038)	1.490 (0.050)	1.493 (0.049)
POr	0.196 (0.013)	0.203 (0.034)	1.428 (0.052)	1.420 (0.044)	0.182 (0.012)	0.185 (0.032)	1.504 (0.049)	1.497 (0.054)
MTG	0.179 (0.013)	0.192 (0.050)	1.499 (0.030)	1.458 (0.038)	0.184 (0.012)	0.197 (0.066)	1.467 (0.033)	1.428 (0.077)
HG	0.195 (0.010)	0.199 (0.018)	1.499 (0.034)	1.466 (0.040)	0.202(0.011)	0.204 (0.015)	1.452 (0.032)	1.426 (0.042)
PT	0.198 (0.013)	0.201 (0.020)	1.477 (0.043)	1.454 (0.037)	0.206 (0.012)	0.210 (0.034)	1.430 (0.032)	1.413 (0.036)
Beijing (N = 50, male = 19, female = 31)								
POp	0.187 (0.014)	0.181 (0.014)	1.444 (0.059)	1.452 (0.049)	0.183 (0.010)	0.177 (0.013)	1.462 (0.044)	1.471 (0.039)
PTr	0.190 (0.012)	0.184 (0.015)	1.406 (0.060)	1.415 (0.045)	0.181 (0.011)	0.177 (0.014)	1.433 (0.062)	1.442 (0.049)
POr	0.196 (0.014)	0.196 (0.018)	1.378 (0.053)	1.376 (0.049)	0.177 (0.017)	0.177 (0.017)	1.467 (0.071)	1.467 (0.051)
MTG	0.187 (0.012)	0.185 (0.017)	1.439 (0.039)	1.431 (0.028)	0.194 (0.010)	0.191 (0.013)	1.415 (0.043)	1.418 (0.034)
HG	0.201 (0.012)	0.191 (0.013)	1.346 (0.050)	1.361 (0.030)	0.205 (0.013)	0.199 (0.013)	1.312 (0.046)	1.331 (0.040)
PT	0.197 (0.010)	0.185 (0.012)	1.394 (0.034)	1.408 (0.029)	0.194 (0.010)	0.193 (0.012)	1.371 (0.032)	1.383 (0.040)

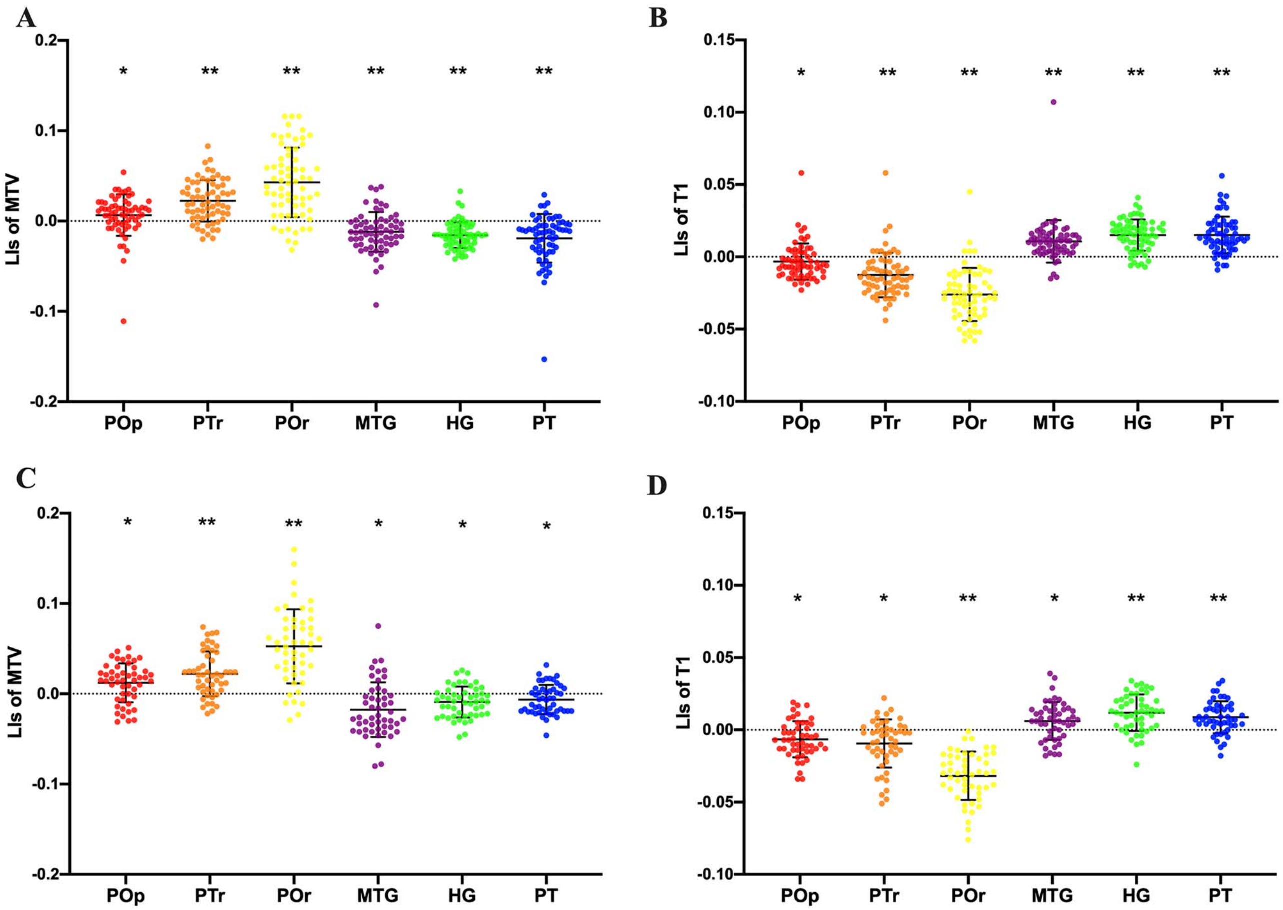

Figure 2. LI of qMRI measures in each ROI. (A) LIs of MTV within each ROI in Guangzhou. (B) LIs of T1 within each ROI in Guangzhou. (C) LIs of MTV within each ROI in Beijing. (D) LIs of T1 within each ROI in Beijing. The error bars indicate standard deviations. POp, pars opercularis; PTr, pars triangularis; POr, pars orbitalis; HG, Heschl's gyrus; PT, planum temporale; MTG, middle temporal gyrus. *$P < 0.05$, **$P < 0.0001$.

Table 3 The percentage of individuals who showed leftward/rightward lateralization in each ROI

	ROI	Guangzhou ($N = 65$)		Beijing ($N = 50$)	
		MTV	T1	MTV	T1
Left-lateralized	POp	62%	62%	72%	72%
	PTr	76%	78%	80%	68%
	POr	82%	90%	88%	100%
Right-lateralized	MTG	68%	90%	76%	72%
	HG	86%	86%	70%	82%
	PT	76%	90%	60%	80%

remove field inhomogeneities, four spin-echo inversion recovery (SEIR) images were scanned, with an echo-planar imaging (EPI) read-out, a slab inversion pulse, and spectral fat suppression. The images were collected with inversion times of 50, 200, 400, 1200, and 2400 ms (TE = 43 ms, TR = 3000 ms) at an in-plane resolution of 2×2 mm^2 with a slice thickness of 4 mm.

Data Analysis

To investigate whether the aforementioned pattern of lateralization would be replicable, the same qMRI data analysis and statistical analysis were conducted on Beijing data.

To examine the myelination-behavior relationship, we used the Spearman correlation to compute the correlation between language task performance (phoneme awareness tasks and tone awareness tasks described below) and microstructural measurements (i.e. MTV and T1) within each ROI on both hemispheres. We also examine the correlation between language task performance and lateralization measurements (i.e. LI and difference percentage) within each ROI. Three participants failed to complete the phoneme awareness tasks. The tone awareness tasks were performed a few months after the brain scan and then only 12 participants helped complete the task.

Behavioral Tasks

Phonological awareness task. Two phonological awareness tasks were used in experiment 1: phoneme counting task and phoneme deletion task. These tasks were presented in English.

(1) Phoneme counting task

Participants were instructed to answer the number of phonemes a word contains after they heard an English word read out by the experimenter (e.g. the word ‘cake’ contains 3 phonemes, /k/, / eI/, and / k/). Thirty words were administered to the participants individually. Response accuracy was recorded by the experimenter.

(2) Phoneme deletion task

Participants were instructed to delete a specific phoneme from a word they heard and then pronounced the rest of the word (e.g. the phoneme /p/ was required to be deleted from the word ‘pear’, the right answer is / e∂/). Each participant completed 30 words, and the accurate rate of the 30 answers was recorded.

Tone awareness task. Three tone awareness tasks were used in experiment 1: monosyllable task, bisyllabic words task, and quadrisyllabic Chinese phrases task. Three types of auditory stimuli were prepared: monosyllable, bisyllabic words, and quadrisyllabic Chinese phrases. All stimuli were orally produced by a professional male announcer (27 years old) in Mandarin at a normal speaking rate. All stimuli were typed in Chinese characters and *pinyin* orthography. Recordings were made in a soundproof booth using a Neumann M149 microphone and a Cubase 9.5 pro software. The announcer sat and the microphone was maintained at a distance of 12 cm from his lip. The stimuli were then edited using Adobe Audition software 7.0 (Adobe Systems, Inc.) to achieve a constant duration for each type of stimuli: 500 ms for monosyllable; 1000 mm for bisyllabic words, and 1900 ms for quadrisyllabic Chinese phrases. These edited stimuli were used in the following three tasks.

(1) *Monosyllable task*

In each trial, participants heard a sequence of three monosyllables and were asked which of the three monosyllables differ from the others in terms of their tones. The onset and rhyme of three items in each trial were entirely distinct from one another. There were 50 trials in this task. The accurate rate of each participant was recorded.

(2) *Bisyllabic words task*

In each trial, participants were asked whether the tones of the two syllables were the same (e.g. /sheng1/ /yin1/, sound) or different (e.g. /jie2/ /gou4/, structure). The bisyllabic words included highly used verbs, adjectives, and nouns with the frequency of occurrence not fewer than 90 per million according to the Modem Chinese Frequency Dictionary. To avoid sandhi effect, tone 3 was excluded for the same-tone trials. All four tones were included in different-tone trials. There were 50 trials in total, 25 for same tone and 25 for different tone. The accurate rate of each participant was recorded.

(3) *Quadrisyllabic Chinese phrases task*

In each trial, participants were asked whether the ending of a quadrisyllabic Chinese phrase is in an incongruous tone. In incongruous-trials, the ending of quadrisyllabic Chinese phrase had the same onset and rhyme as the conventional one. The quadrisyllabic Chinese phrases were also highly used. Thirty-three participants who were native to the purpose of the experiment were asked to give the phonetic notation of each character in each quadrisyllabic Chinese phrase and the average accuracy was 94.85%. There were 50 trials in total, 25 for congruous-tone and 25 for incongruous-tone. The accurate rate of each participant was recorded.

Results

LIs of MTV were significantly larger than zero in inferior frontal areas including the POp [$Z = 3.375$, $p_{corr} = 0.0011$, $M = 0.0121$, $SD = 0.0216$, 95%CI = [0.0060, 0.0183], effect size = 0.48], PTr

[$Z = 4.939$, $p_{corr} < 0.0001$, $M = 0.0220$, SD = 0.0249, 95%CI = [0.0151, 0.0292], effect size = 0.70], and POr [$Z = 5.797$, $p_{corr} < 0.0001$, $M = 0.0526$, SD = 0.0410, 95%CI = [0.0409, 0.0642], effect size = 0.82], indicating a reliable left lateralization. LIs of MTV were significantly smaller than zero in temporal areas including the MTG [$Z = -3.842$, $p_{corr} = 0.0002$, $M = -0.0176$, SD = 0.0301, 95%CI = [−0.0262, −0.0090], effect size = 0.54], HG [$Z = -3.348$, $p_{corr} = 0.0010$, $M = -0.0091$, SD = 0.0170, 95%CI = [−0.0139, −0.0042], effect size = 0.47], and PT [$Z = -2.643$, $p_{corr} = 0.0008$, $M = -0.0063$, SD = 0.0162, 95%CI = [−0.0109, −0.0017], effect size = 0.37], showing a reliable rightward lateralization (see Fig. 2C).

In addition, LIs of T1 were significantly smaller than zero in inferior frontal areas including the POp [$Z = -3.264$, $p_{corr} = 0.0013$, $M = -0.0066$, SD =0.0126, 95%CI = [−0.0101, −0.0030], effect size = 0.46], PTr [$Z = -3.464$, $p_{corr} = 0.0008$, $M = -0.0095$, SD = 0.0166, 95%CI = [−0.0142, −0.0047], effect size = 0.49], and POr [$Z = -6.155$, $p_{corr} < 0.0001$, $M = -0.0318$, SD = 0.0168, 95%CI = [−0.0366, −0.0271], effect size = 0.87], but were significantly larger than zero in temporal areas including the MTG [$Z = 2.931$, $p_{corr} = 0.0034$, $M = 0.0061$, SD = 0.0131, 95%CI = [0.0024, 0.0099], effect size = 0.41], HG [$Z = 4.965$, $p_{corr} < 0.0001$, $M = 0.0118$, SD = 0.0126, 95%CI = [0.0083, 0.0154], effect size = 0.70] and PT [$Z = 4.558$, $p_{corr} < 0.0001$, $M = 0.0088$, SD = 0.0110, 95%CI = [0.0056, 0.0119], effect size = 0.64] (see Fig. 2D).

The difference percentage of MTV and T1 showed the same lateralization patterns as LI of MTV and T1 (Fig. S1C&D). Specifically, MTV in Pop, PTr, and POr was 2.6%, 4.6%, and 11.5% larger in left than right hemisphere, respectively [POp: $Z = 3.499$, $p_{corr} = 0.0007$; PTr: $Z = 4.947$, $p_{corr} < 0.0001$; POr: $Z = 5.816$, $p_{corr} < 0.0001$], while MTV in MTG, HG, and PT was 3.3%, 1.7%, and 1.2% smaller in left than right hemisphere, respectively [MTG: $Z = -3.721$, $p_{corr} = 0.0004$; HG: $Z = -3.277$, $p_{corr} = 0.0013$; PT: $Z = -2.582$, $p_{corr} = 0.0098$]. In addition, T1 in Pop, PTr, and POr was 1.3%, 1.8%, and 6.1% smaller in left than right hemisphere, respectively [POp: $Z = -3.263$, $p_{corr} = 0.0013$; PTr: $Z = -3.456$, $p_{corr} = 0.0008$; POr: $Z = -6.154$, $p_{corr} < 0.0001$], while T1 in MTG, HG, and PT was 1.3%, 2.4%, and 1.8% larger in left than right hemisphere, respectively [MTG: $Z = 2.973$, $p_{corr} = 0.0029$; HG: $Z = 4.971$, $p_{corr} < 0.0001$; PT: $Z = 4.600$, $p_{corr} < 0.0001$].

Percentages of the individuals in Beijing showing the same lateralization pattern ranged from 60% to 100% (Table 3). No ROI showed a significant gender difference in LI and difference percentage ($ps > 0.05$).

We also collapsed data from Beijing and Guangzhou and conducted the same data analysis on the lateralization measurements (i.e. LI and difference percentage). The results can be found in Table S7.

The demographic information and behavioral performance of participants are illustrated in Table 1. Spearman correlation was performed to examine the relationship between the microstructural measurements (i.e. MTV and T1) and language task performance. The results were shown in Tables S5 and S6. None of the P values in the Spearman correlation was survived from FDR corrections.

Then, we conducted Spearman correlations on LIs of MTV/T1 and language task performance to examine the myelination-behavior relationship from the perspective of laterality index. The results were shown in Tables 4 and 5. Phoneme deletion accuracy showed a significant negative correlation with LI of T1 in POr [$r = -0.327$, $p_{corr} = 0.050$, Fig. 3A]. Phoneme counting accuracy showed significant negative correlations with LI of T1 in POr [$r = -0.420$, $p_{corr} = 0.018$, Fig. 3B]. The bisyllabic words task accuracy showed a significant positive correlation with LI of MTV in POr [$r = 0.747$, $p_{corr} = 0.030$]. Additionally, the correlation between difference percentage of MTV/T1 and language task performance showed similar results (see Table S8–S9). These results indicated that the degree of leftward lateralization is positively related to language skills including phoneme awareness and tone awareness.

Discussion

In the current study, we used the qMRI technique to investigate the myeloarchitectonic asymmetries of language regions as well as the myelination-behavior relationship. A mixed pattern of myeloarchitectonic asymmetries in the living human brain was found. While the lateralization of inferior frontal areas including the pars opercularis, pars triangularis, and pars orbitalis is leftward, that of the middle and superior temporal gyrus (Heschl's gyrus and planum temporale) is rightward. There was no gender difference in lateralization. Moreover, the leftward lateralization of myelination structure is positively related to language skills. In our study, the observed lateralization pattern was reproducible in two cohorts. Our results provided strong evidence that MR data from different instruments can be quite comparable.

Our results of left-lateralized inferior frontal area are consistent with previous findings of area 44 and area 45 at the microstructural level (Bogolepova and Malofeeva 2000, 2001; Uylings et al. 2006). Previous studies showed gender differences in terms of neuronal density and volume based on small sample size ($N < 20$) (Amunts et al. 1999; Bogolepova and Malofeeva 2000, 2001; Uylings et al. 2006). However, in our study, gender difference of microstructural lateralization was not observed in larger subject pools ($N = 65$ and 50).

The right-lateralized myelination structure observed in the temporal areas in our study appears to be inconsistent with much of the prior data. Anderson et al. (1999) found that axons of posterior superior temporal lobe had thicker myelin sheaths on the left side than on the right side. However, the results came from eight subjects whose axons were observed by electron microscopy. Other studies that measured clusters spacing (Galuske et al. 2000) and pyramidal cell size (Hutsler and Galuske 2003; Hutsler 2003) only provide fractional features of microstructure, which cannot reflect the myelination structure as in our study. They are also severely limited by the sample composition, sample size, and location of cells that can be stained. The myeloarchitectonic asymmetries measured quantitatively in our study reflected a general asymmetry of language processing. Although the lateralization measurements (i.e. LI and difference percentage) indicated a rightward myelination structure within temporal area, we found a relationship between leftward lateralization of temporal area and language skills.

It has been suggested that the processing of phonemes in one's native language is left lateralized, whereas detection of prosody is right lateralized (Minagawa-Kawai et al. 2011). However, in our study, participants' performance of tone awareness task, as well as phoneme awareness task, were both related to leftward asymmetry values. We should note that the correlations between lateralization measurements and language skills found in our study do not ensure a causal relationship, and it should be cautious to interpret our data as being predictive of participants' reading and language test scores. Future research should investigate the possibility of different cortical myeloarchitectonic asymmetry patterns across cultures, and how these asymmetries may be associated with brain activations in

Table 4 Correlation between LI of MTV/T1 in each ROI and phoneme awareness task performance ($N = 47$)

		Phoneme deletion task		Phoneme counting task	
		r	Corrected *P*	*r*	Corrected *P*
LI of MTV	POp	0.316	0.093	0.105	0.483
	PTr	0.283	0.065	0.181	0.448
	POr	0.284	0.080	0.221	0.816
	MTG	0.125	0.403	0.218	0.426
	HG	0.289	0.098	0.144	0.403
	PT	0.326	0.150	0.171	0.377
LI of T1	POp	−0.226	0.127	−0.138	0.426
	PTr	−0.363	0.072	−0.234	0.228
	POr	−0.327*	0.050	−0.420*	0.018
	MTG	−0.346	0.051	−0.301	0.120
	HG	−0.305	0.056	−0.181	0.333
	PT	−0.294	0.054	−0.088	0.557

Note: *corrected $P < 0.05$

Table 5 Correlation between LI of MTV/T1 in each ROI and tone awareness task performance ($N = 12$)

		Monosyllable task		Bisyllabic words task		Quadrisyllabic Chinese phrases task	
		r	corrected *P*	*r*	corrected *P*	*r*	corrected *P*
LI of MTV	POp	−0.213	0.761	0.007	0.983	−0.189	0.834
	PTr	0.071	0.827	0.209	0.773	−0.315	0.954
	POr	0.454	0.828	0.747*	0.030	0.000	1.000
	MTG	−0.184	0.679	−0.042	1.075	−0.101	0.906
	HG	0.340	0.837	0.432	0.483	−0.454	0.828
	PT	0.277	0.768	0.375	0.458	−0.202	1.060
LI of T1	POp	0.310	1.962	0.014	0.965	0.291	0.539
	PTr	−0.075	0.818	−0.232	1.404	0.404	0.579
	POr	−0.099	1.518	−0.450	0.858	0.046	0.887
	MTG	0.203	1.584	0.069	0.997	0.309	0.656
	HG	0.078	0.972	−0.209	1.030	0.593	0.252
	PT	0.085	1.188	−0.124	1.052	0.255	0.509

Note: *corrected $P < 0.05$

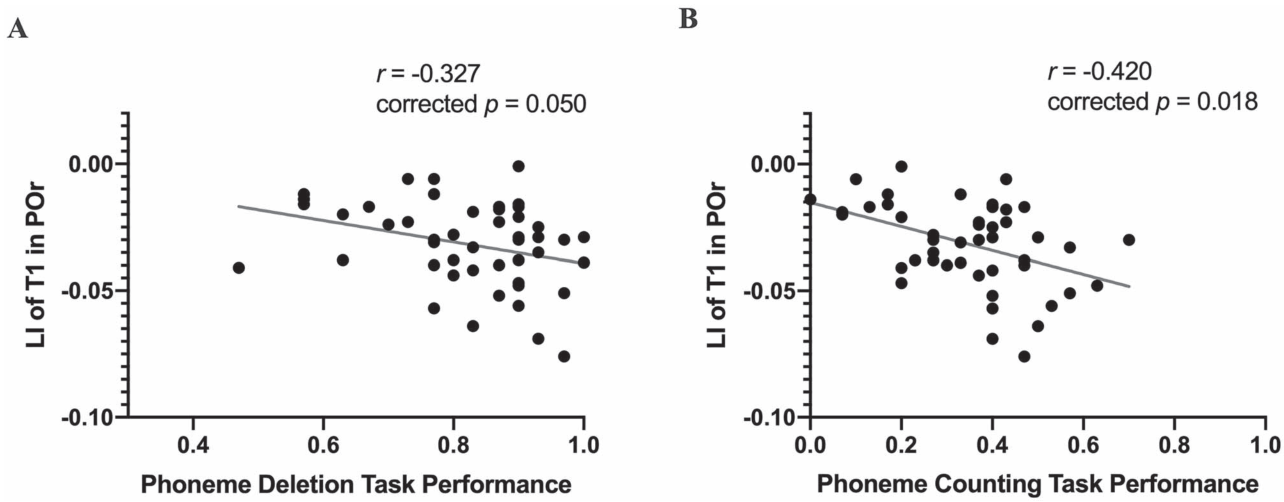

Figure 3. Myeloarchitectonic asymmetry and language task performance. (A) The correlation between the phoneme deletion task performance and LIs of T1 in POr. (B) The correlation between the phoneme counting task performance and LIs of T1 in POr.

language tasks and with language impairments such as stuttering and dyslexia.

Supplementary Material

Supplementary material can be found at *Cerebral Cortex* online.

Notes

We thank Joey Tang and Chunqi Chang for their constructive comments. Please send correspondence to: Dr. Li Hai Tan at tanlh@sions.cn, Dr. Shijun Qiu at qiu-sj@163.com, or Dr. Jia-Hong Gao at jgao@pku.edu.cn. *Conflict of Interest*: The authors declare no competing financial interests.

Funding

This work was supported by Guangdong Key Basic Research Grant (2018B030332001), Guangdong Pearl River Talents Plan (2016ZT06S220), Shenzhen Peacock Plan (KQTD2015033016104926), and Shenzhen Basic Research Scheme (JCYJ20170818110103216, JCYJ20170412164259361, JCYJ20170818110022721, JCYJ20170412-164413575).

References

Amunts K. 2010. Structural indices of asymmetry. In: *The two halves of the brain*. Cambridge: MIT Press, pp. 145–176.

Amunts K, Schleicher A, Bürgel U, Mohlberg H, Uylings HB, Zilles K. 1999. Broca's region revisited: cytoarchitecture and intersubject variability. *J Comp Neurol*. 412:319–341.

Anderson B, Southern BD, Powers RE. 1999. Anatomic asymmetries of the posterior superior temporal lobes: a postmortem study. *Neuropsychiatry Neuropsychol Behav Neurol*. 12:247.

Barral JK, Gudmundson E, Stikov N, Etezadi-Amoli M, Stoica P, Nishimura DG. 2010. A robust methodology for in vivo T1 mapping. *Magn Reson Med*. 64:1057–1067.

Barrick T, Lawes I, Clark C, editors. 2004. White matter pathway asymmetry corresponds to auditory-spatial and language lateralisation. *J Anat*. 204:230–231.

Barrick TR, Lawes IN, Mackay CE, Clark CA. 2007. White matter pathway asymmetry underlies functional lateralization. *Cereb Cortex*. 17:591–598.

Benjamini Y, Hochberg Y. 1995. Controlling the false discovery rate: a practical and powerful approach to multiple testing. *Journal of the Royal Statistical Society: Series B (Methodological)*. 57:289–300.

Berl MM, Mayo J, Parks EN, Rosenberger LR, VanMeter J, Ratner NB, Vaidya CJ, Gaillard WD. 2014. Regional differences in the developmental trajectory of lateralization of the language network. *Hum Brain Mapp*. 35:270–284.

Binder JR, Frost JA, Hammeke TA, Rao SM, Cox RW. 1996. Function of the left planum temporale in auditory and linguistic processing. *Brain*. 119:1239–1247.

Bishop DVM. 2013. Cerebral asymmetry and language development: cause, correlate, or consequence? *Science*. 340:1230531.

Bogolepova I, Malofeeva L. 2000. The developmental characteristics of speech-motor areas 44 and 45 in the left and right hemispheres of the human brain in early postnatal development. *Morfologiia (Saint Petersburg, Russia)*. 117:13–18.

Bogolepova I, Malofeeva L. 2001. Characteristics of the development of speech motor areas 44 and 45 in the left and right hemispheres of the human brain in early post-natal ontogenesis. *Neurosci Behav Physiol*. 31:349–354.

Broca P. 1861. Remarques sur le siège de la faculté du langage articulé, suivies d'une observation d'aphémie (perte de la parole). *Bulletin et Memoires de la Societe anatomique de Paris*. 6:330–357.

Cao F, Wang Z, Sussman BL, Yan X, Spray GJ, Rios V. 2019. L1 Reading experience influences L2 lexical learning: Spanish learning in Chinese speakers and English speakers. *Neuroscience*. 416:255–267.

Chang HC, Lee HJ, Tzeng OJ, Kuo WJ. 2014. Implicit target substitution and sequencing for lexical tone production in Chinese: an fMRI study. *PloS One*. 9:e83126.

Destrieux C, Fischl B, Dale A, Halgren E. 2010. Automatic parcellation of human cortical gyri and sulci using standard anatomical nomenclature. *Neuroimage*. 53:1–15.

Dorsaint-Pierre R, Penhune VB, Watkins KE, Neelin P, Lerch JP, Bouffard M, Zatorre RJ. 2006. Asymmetries of the planum temporale and Heschl's gyrus: relationship to language lateralization. *Brain*. 129:1164–1176.

Falzi G, Perrone P, Vignolo LA. 1982. Right-left asymmetry in anterior speech region. *Arch Neurol*. 39:239–240.

Fischl B, Van Der Kouwe A, Destrieux C, Halgren E, Ségonne F, Salat DH, Busa E, Seidman LJ, Goldstein J, Kennedy D. 2004. Automatically parcellating the human cerebral cortex. *Cereb Cortex*. 14:11–22.

Foundas AL, Eure KF, Luevano LF, Weinberger DR. 1998. MRI asymmetries of Broca's area: the pars triangularis and pars opercularis. *Brain Lang*. 64:282–296.

Fram EK, Herfkens RJ, Johnson GA, Glover GH, Karis JP, Shimakawa A, Perkins TG, Pelc NJ. 1987. Rapid calculation of T1 using variable flip angle gradient refocused imaging. *Magn Reson Imaging*. 5:201–208.

Frost JA, Binder JR, Springer JA, Hammeke TA, Bellgowan PS, Rao SM, Cox RW. 1999. Language processing is strongly left lateralized in both sexes: evidence from functional MRI. *Brain*. 122:199–208.

Galuske RA, Schlote W, Bratzke H, Singer W. 2000. Interhemispheric asymmetries of the modular structure in human temporal cortex. *Science*. 289:1946–1949.

Gandour J, Wong D, Hsieh L, Weinzapfel B, Van Lancker D, Hutchins GD. 2000. A crosslinguistic PET study of tone perception. *J Cogn Neurosci*. 12:207–222.

Ge J, Peng G, Lyu B, Wang Y, Zhuo Y, Niu Z, Tan LH, Leff AP, Gao JH. 2015. Cross-language differences in the brain network subserving intelligible speech. *Proc Natl Acad Sci USA*. 112:2972–2977.

Geschwind N, Galaburda AM. 1985. Cerebral lateralization: biological mechanisms, associations, and pathology: I. a hypothesis and a program for research. *Arch Neurol*. 42:428–459.

Geschwind N, Levitsky W. 1968. Human brain: left-right asymmetries in temporal speech region. *Science*. 161:186–187.

Gomez J, Barnett MA, Natu V, Mezer A, Palomero-Gallagher N, Weiner KS, Amunts K, Zilles K, Grill-Spector K. 2017. Microstructural proliferation in human cortex is coupled with the development of face processing. *Science*. 355:68–71.

Greve DN, Lise VDH, Qing C, Steven S, Sabuncu MR, Bruce F, Marc B. 2013. A surface-based analysis of language lateralization and cortical asymmetry. *J Cognitive Neurosci*. 25: 1477–1492.

Hsieh L, Gandour J, Wong D, Hutchins GD. 2001. Functional heterogeneity of inferior frontal gyrus is shaped by linguistic experience. *Brain Lang*. 76:227–252.

Hugdahl K, Westerhausen R. 2010. *The two halves of the brain: Information processing in the cerebral hemispheres*. Cambridge: MIT Press.

Hutsler J, Galuske RAW. 2003. Hemispheric asymmetries in cerebral cortical networks. *Trends Neurosci*. 26:429–435.

Hutsler JJ. 2003. The specialized structure of human language cortex: pyramidal cell size asymmetries within auditory and language-associated regions of the temporal lobes. *Brain Lang*. 86:226–242.

Keller SS, Crow T, Foundas A, Amunts K, Roberts N. 2009. Broca's area: nomenclature, anatomy, typology and asymmetry. *Brain Lang*. 109:29–48.

Klein D, Zatorre RJ, Milner B, Zhao V. 2001. A cross-linguistic PET study of tone perception in Mandarin Chinese and English speakers. *Neuroimage*. 13:646–653.

Knecht S, Deppe M, Dräger B, Bobe L, Lohmann H, Ringelstein E-B, Henningsen H. 2000. Language lateralization in healthy right-handers. *Brain*. 123:74–81.

Kwok VPY, Dan G, Yakpo K, Matthews S, Tan LH. 2016. Neural systems for auditory perception of lexical tones. *J. Neurolinguistics*. 37:34–40.

Kwok VPY, Dan G, Yakpo K, Matthews S, Fox PT, Li P, Tan LH. 2017. A meta-analytic study of the neural systems for auditory processing of lexical tones. *Front Hum Neurosci*. 11:375.

Lattner S, Meyer ME, Friederici AD. 2005. Voice perception: sex, pitch, and the right hemisphere. *Hum Brain Mapp*. 24:11–20.

Li X, Gandour JT, Talavage T, Wong D, Hoffa A, Lowe M, Dzemidzic M. 2010. Hemispheric asymmetries in phonological processing of tones vs. segmental units. *Neuroreport*. 21:690.

Liang B, Du Y. 2018. The functional neuroanatomy of lexical tone perception: an activation likelihood estimation meta-analysis. *Front Neurosci*. 12:495.

Liu L, Peng D, Ding G, Jin Z, Zhang L, Li K, Chen C. 2006. Dissociation in the neural basis underlying Chinese tone and vowel production. *Neuroimage*. 29:515–523.

Liu C, Zhang WT, Tang YY, Mai XQ, Chen HC, Tardif T, Luo YJ. 2008. The visual word form area: evidence from an fMRI study of implicit processing of Chinese characters. *Neuroimage*. 40:1350–1361.

Luo D, Kwok VPY, Liu Q, Li W, Yang Y, Zhou K, Xu M, Gao JH, Tan LH. 2019. Microstructural plasticity in the bilingual brain. *Brain Lang*. 196:104654.

Luo H, Ni JT, Li ZH, Li XO, Zhang DR, Zeng FG, Chen L. 2006. Opposite patterns of hemisphere dominance for early auditory processing of lexical tones and consonants. *Proc Natl Acad Sci USA*. 103:19558–19563.

Lutti A, Dick F, Sereno MI, Weiskopf N. 2014. Using high-resolution quantitative mapping of R1 as an index of cortical myelination. *Neuroimage*. 93:176–188.

Mei L, Xue G, Lu ZL, Chen C, Wei M, He Q, Dong Q. 2015. Long-term experience with Chinese language shapes the fusiform asymmetry of English reading. *Neuroimage*. 110:3–10.

Mezer A, Rokem A, Berman S, Hastie T, Wandell BA. 2016. Evaluating quantitative proton-density-mapping methods. *Hum Brain Mapp*. 37:3623–3635.

Mezer A, Yeatman JD, Stikov N, Kay KN, Cho NJ, Dougherty RF, Perry ML, Parvizi J, Hua LH, Butts-Pauly K, et al. 2013. Quantifying the local tissue volume and composition in individual brains with magnetic resonance imaging. *Nat Med*. 19:1667–1672.

Minagawa-Kawai Y, Cristià A, Dupoux E. 2011. Cerebral lateralization and early speech acquisition: a developmental scenario. *Dev Cogn Neuros*. 1:217–232.

Nan Y, Friederici AD. 2013. Differential roles of right temporal cortex and Broca's area in pitch processing: evidence from music and Mandarin. *Hum Brain Mapp*. 34:2045–2054.

Oishi H, Takemura H, Aoki SC, Fujita I, Amano K. 2018. Microstructural properties of the vertical occipital fasciculus explain the variability in human stereoacuity. *Proc Natl Acad Sci USA*. 115:12289–12294.

Olulade OA, Seydell-Greenwald A, Chambers CE, Turkeltaub PE, Dromerick AW, Berl MM, Gaillard WD, Newport EL. 2020. The neural basis of language development: changes in lateralization over age. *Proc Natl Acad Sci USA*. 117:23477–23483.

Penhune V, Zatorre R, MacDonald J, Evans A. 1996. Interhemispheric anatomical differences in human primary auditory cortex: probabilistic mapping and volume measurement from magnetic resonance scans. *Cereb Cortex*. 6:661–672.

Pylkkänen L. 2019. The neural basis of combinatory syntax and semantics. *Science*. 366:62–66.

Ren GQ, Yang Y, Li X. 2009. Early cortical processing of linguistic pitch patterns as revealed by the mismatch negativity. *Neuroscience*. 162:87–95.

Reuter M, Schmansky NJ, Rosas HD, Fischl B. 2012. Within-subject template estimation for unbiased longitudinal image analysis. *Neuroimage*. 61:1402–1418.

Rodd JM, Vitello S, Woollams AM, Adank P. 2015. Localising semantic and syntactic processing in spoken and written language comprehension: an activation likelihood estimation meta-analysis. *Brain Lang*. 141:89–102.

Shaywitz BA, Shaywitz SE, Pugh KR, Constable RT, Skudlarski P, Fulbright RK, Bronen RA, Fletcher JM, Shankweller DP, Katz L, et al. 1995. Sex differences in the functional organization of the brain for language. *Nature*. 373:607–609.

Snyder PJ, Harris LJ. 1993. Handedness, sex, and familial sinistrality effects on spatial tasks. *Cortex*. 29:115–134.

Steinmetz H, Rademacher J, Huang Y, Hefter H, Zilles K, Thron A, Freund H-J. 1989. Cerebral asymmetry: MR planimetry of the human planum temporale. *J Comput Assist Tomogr*. 13:996–1005.

Stüber C, Morawski M, Schäfer A, Labadie C, Wähnert M, Leuze C, Streicher M, Barapatre N, Reimann K, Geyer S. 2014. Myelin and iron concentration in the human brain: a quantitative study of MRI contrast. *Neuroimage*. 93:95–106.

Takao H, Abe O, Yamasue H, Aoki S, Sasaki H, Kasai K, Yoshioka N, Ohtomo K. 2011. Gray and white matter asymmetries in healthy individuals aged 21–29 years: a voxel-based morphometry and diffusion tensor imaging study. *Hum Brain Mapp*. 32:1762–1773.

Tan LH, Chen L, Yip V, Chan AH, Yang J, Gao JH, Siok WT. 2011. Activity levels in the left hemisphere caudate–fusiform circuit predict how well a second language will be learned. *Proc Natl Acad Sci USA*. 108:2540–2544.

Tan LH, Liu H-L, Perfetti CA, Spinks JA, Fox PT, Gao J-H. 2001. The neural system underlying Chinese logograph reading. *Neuroimage*. 13:836–846.

Tremblay P, Dick AS. 2016. Broca and Wernicke are dead, or moving past the classic model of language neurobiology. *Brain Lang*. 162:60–71.

Uylings H, Malofeeva L, Bogolepova I, Jacobsen A, Amunts K, Zilles K. 2005. No postnatal doubling of number of neurons in human Broca's areas (Brodmann areas 44 and 45)? A stereological study. *Neuroscience*. 136:715–728.

Uylings HB, Jacobsen AM, Zilles K, Amunts K. 2006. Left-right asymmetry in volume and number of neurons in adult Broca's area. *Cortex*. 42:652–658.

Wada JA, Clarke R, Hamm A. 1975. Cerebral hemispheric asymmetry in humans: cortical speech zones in 100 adult and 100 infant brains. *Arch Neurol*. 32:239–246.

Wernicke C, editor. 1969. The symptom complex of aphasia, *Proceedings of the Boston Colloquium for the Philosophy of Science 1966/1968*; Dordrecht: Springer. p. 34–97.

Wildgruber D, Riecker A, Hertrich I, Erb M, Grodd W, Ethofer T, Ackermann H. 2005. Identification of emotional intonation evaluated by fMRI. *Neuroimage*. 24:1233–1241.

Witelson SF, Glezer II, Kigar DL. 1995. Women have greater density of neurons in posterior temporal cortex. *J Neurosci*. 15:3418–3428.

Witelson SF, Kigar DL. 1988. *Asymmetry in Brain Function Follows Asymmetry in Anatomical Form: Gross, Microscopic, Postmortem and Imaging Studies*. Amsterdam: Elsevier Science

Wong PCM. 2002. Hemispheric specialization of linguistic pitch patterns. *Brain Res Bull*. 59:83–95.

Xi J, Zhang LJ, Shu H, Zhang Y, Li P. 2010. Categorical perception of lexical tones in Chinese revealed by mismatch negativity. *Neuroscience*. 170:223–231.

Xue G, Chen C, Jin Z, Dong Q. 2006. Cerebral asymmetry in the fusiform areas predicted the efficiency of learning a new writing system. *J Cog Neurosci*. 18:923–931.

Xue G, Dong Q, Chen K, Jin Z, Chen C, Zeng Y, Reiman EM. 2005. Cerebral asymmetry in children when reading Chinese characters. *Cognitive Brain Research*. 24:206–214.

Yang Y, Zuo Z, Tam F, Graham SJ, Tao R, Wang N, Bi H-Y. 2019. Brain activation and functional connectivity during Chinese writing: an fMRI study. *J Neurolinguist*. 51:199–211.

Yip M. 2002. *Tone*. Cambridge: CUP.

Yu K, Wang R, Li L, Li P. 2014. Processing of acoustic and phonological information of lexical tones in mandarin Chinese revealed by mismatch negativity. *Front Hum Neurosci*. 8:729.